COBEM 2021 26th International Congress of Mechanical Engineering
November 22-26, 2021, Virtual Congress, Brazil

COB-2021-2262
THERMAL ANALYSIS OF A PERMANENT MAGNET SYNCHRONOUS GENERATOR FOR A 10 MW WIND TURBINE

Gabriel Fernandes Bravo
Marcos Vinício Oro
Matheus Protasio de Lima
Edson Bazzo
Universidade Federal de Santa Catarina, Campus Universitário Reitor João David Ferreira Lima, s/nº Trindade, Florianópolis, SC
gabriel.f.bravo@labcet.ufsc.br
oro@labcet.ufsc.br
matheus.protasio@labcet.ufsc.br
e.bazzo@ufsc.br

Abstract. *The offshore environment provides not only more consistent, stronger, and less turbulent winds with smaller shear but also logistical advantages. Besides, noise and visual problems are avoided, depending on the distance from the coast. Therefore, the use of offshore wind generators has grown over the last few years, and, in this context, direct-drive permanent magnet synchronous generators (DD-PMSG) are an attractive topology, since less maintenance is required, due to gearbox elimination. To ensure that the generator is working safely – mostly because of winding and permanent magnet temperature limits – thermal control is required. Thus, this work presents the thermal behavior analysis of a 10 MW inner rotor DD-PMSG. The main losses - mostly through copper, iron, and magnets - were estimated and used as input data for the lumped parameter model with forced air cooling on the outer surface of the stator, which led to extreme temperatures. Therefore, the cooling strategy was changed for direct water cooling and simulated for a range of flow rates. Direct cooling consists of water channels coils inside the winding, which is the main source of energy losses. Direct cooling achieved safe conditions reaching efficiency of about 91.5 % for a cooling system of 20 passes and total flow rate of 1600 L/min.*

Keywords: *PMSG, Heat Transfer, Lumped Parameter, Wind Energy, Direct Drive*

1. INTRODUCTION

Wind power is one of the most promising renewable energy sources and plays an important role in the energy transition, especially replacing fossil fuels. In 2020 renewables generated in the European Union more electricity than fossil fuels for the first time, mainly powered by 14.7 GW of new wind facilities connected to the grid (GWEC, 2021).

Large capacity wind farms are being promoted worldwide, where increasingly larger turbines are being used. In this context, offshore applications reach a prominent place in power generation. The sea-based sites have low surface roughness, allowing steadier and stronger wind profiles. This resource availability promotes the development of turbines with larger capacities. This growth in the power rating carries many challenges, such as the need for more elaborate thermal control techniques.

The heat produced by a wind turbine rises significantly with the increase of the unit capacity of these systems. The main heat-generating components are the gearbox, power converter and generator. In offshore wind turbines, direct-driven (DD) electrical generators have become a promising alternative. These systems enable direct coupling to the turbine blades, eliminating gearboxes. In addition, the permanent magnet synchronous generators (PMSG) have become the major trend in offshore facilities, due to their high reliability, small maintenance and high efficiency (Fan *et al.*, 2019).

However, the DD-PMSG generators present several thermal challenges. The rise in the operating temperature causes demagnetization, damage in the windings and thermal stress in the generator body. In large-scale offshore turbines, the maintenance is not only expensive but also difficult to be performed. Therefore, effective cooling methods are extremely important.

A thermal model of a 500 kW PMSG cooled by forced air convection was proposed by Grauers (1996). In that work, the power losses are estimated using empirical equations and a lumped parameter model calculates the temperature field through a matrix of conductances. That model was employed in several recent works, such as Bazzo *et al.* (2015), and Moghadam and Nejad (2020). Although the aforementioned work has considered air cooling, Jiang (2010) states that in wind systems with power beyond 750 kW, liquid cooling should be implemented to supply the thermal requirements.

Different cooling strategies are found in the technical literature. Alexandrova *et al.* (2014) presented results for an 8

MW DD-PMSG that uses direct liquid cooling. The stator winding was cooled by deionized water, which flows through a hollow conductor stated as tooth-coil, where the winding is embedded. A lumped-parameter thermal model and finite element analysis were performed to predict the temperature distributions for the generator. The models were validated by comparing results to experimental data. Fan *et al.* (2019) studied the thermal performance of the cooling system for 3.2 MW split-type DD-PMSG. Three schemes were investigated: (a) stator pipeline-circulating water-cooling, (b) shell-type water-cooling and (c) stator-slot air-cooling. Computational Fluid Dynamics was employed to perform the calculations. Both water-cooled schemes presented better performances than the air-cooled system.

Here, the thermal losses and the temperature distribution of a 10 MW DD-PMSG are investigated. The lumped parameter network thermal model (LPN) proposed by Grauers (1996) was extended to include the liquid forced convection as cooling strategy. Direct liquid cooling is compared to external forced air convection. In addition, a model of multiple passes of water channels is implemented.

2. CASE STUDY

2.1 Studied generator

This study used the electric generator presented by Moghadam and Nejad (2020), which performed an optimization to design a DD-PMSG to minimize the generator cost and maximize the electromagnetic torque density. The generator is a three-phase radial flux machine with inner rotor. The armature windings are placed in slots in the iron core, where each slot has two layers. The magnets are of NdFeB material and placed on the rotor surface. The slot height was the only modified dimension from the original design, which was performed to include the cooling channel, as presented in section 2.2. The main technical specifications are summarised in Tab. 1. This generator is a three-phase radial flux machine with inner rotor. The armature windings are placed in slots in the iron core, where each slot has two layers. The magnets are of NdFeB material and placed on the rotor surface.

Table 1. Technical Specifications of the studied generator

Technical Specifications	
Number of poles	200
Rated output power P_{out}, MW	10.0
Rated rotational speed n_r, rpm	9.60
Rated generator output frequency f, Hz	16.00
Current density J_s, A/mm^2	4.66
Rated RMS line voltage V_L, V	3471
Maximum air-gap flux density $\hat{B}_\delta$, T	0.46
Maximum magnet flux density $\hat{B}_m$, T	0.48
Maximum stator teeth flux density $\hat{B}_t$, T	0.95
Maximum stator yoke flux density $\hat{B}_{sy}$, T	1.10
Maximum rotor yoke flux density $\hat{B}_{sy}$, T	1.10
Air gap diameter D_s, m	10.62

2.2 Proposed cooling systems

In this work, two cooling strategies are studied. In the first one, it is considered forced air convection directly on the stator core outer surface, as proposed by Grauers (1996), wherein external fans pump ambient air around the stator circumference, providing air at 15 m/s and a convection heat transfer of 60 W/m^2K. In the second one, it is proposed a liquid cooling strategy, as shown in Fig. 1. Water is pumped through a rectangular channel placed between the layers of the slot. The channel has an external height of 5 mm, an external width of 27.4 mm, and a wall thickness of 1 mm. In this way, the copper windings are cooled directly by liquid convection. The pipeline crosses the generator length in each slot. A set of channels are connected in series comprising a cooling coil. The coils are assembled in parallel covering all slots of the generator. A study of the temperature behavior for a different number of passes in the cooling coil is performed.

3. METHODOLOGY

3.1 Losses calculation

In order to obtain the thermal field, losses need to be evaluated. For a permanent magnet synchronous generator, the main loss is through copper in the stator, dependent on armature current and copper temperature. Other losses include

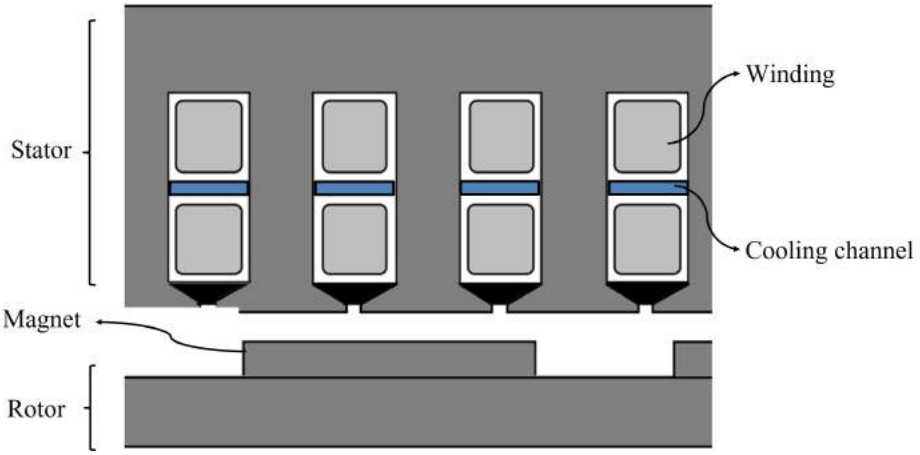

Figure 1. Proposed liquid cooling system.

stator hysteresis and eddy current losses, function of flux linkage and frequency, and friction losses, dependent of generator rotation speed. Furthermore, thermal losses through the permanent magnet are also evaluated. Grauers (1996) presents the equations to evaluate the specific losses, that is, per unit mass. Therefore, the generator geometry needs to be completely defined. The losses data are then used as input to evaluate the thermal field.

3.2 Lumped parameter thermal model

The model proposed by Grauers (1996) aims to evaluate the hottest parts of the generator, such as copper winding and magnets, and it was designed combining a detailed model, which was based on one slot pitch, one rotor pole, one coil, internal air, and end shield, in a simplified model for n_s slots and coils. External forced air convection is performed on the stator outer surface. The model assumes heat flow to be bidimensional in the iron core and tridimensional in the coils. The simplified generator thermal circuit of the slot pitch is shown in Fig. 2a and a representation of the complete simplified model is shown in Fig. 2b.

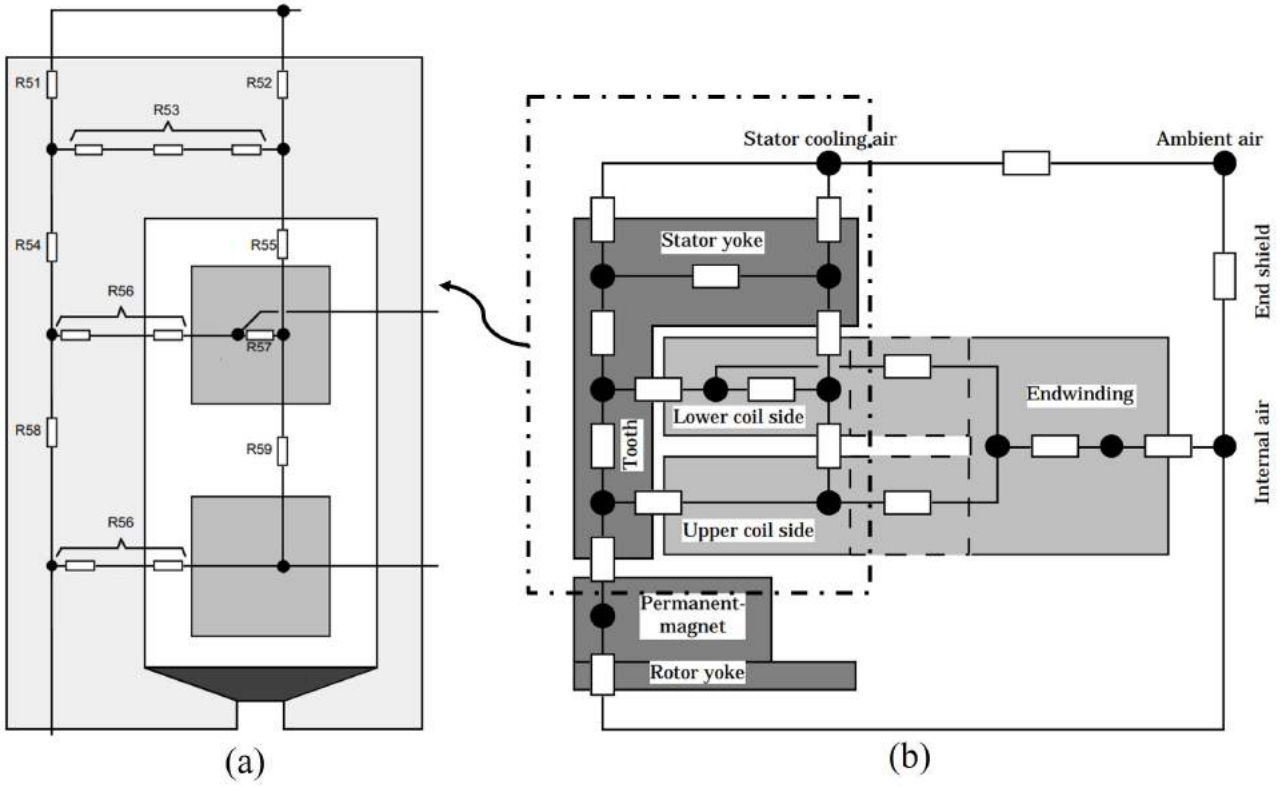

Figure 2. Generator thermal model: (a) slot simplified circuit; (b) complete simplified circuit (Grauers, 1996)).

The model with direct cooling was adapted from Grauers (1996), wherein water cooling was included between the winding layers, as shown in Fig. 3. Furthermore, on the stator outer surface was considered natural convection instead of forced convection. In this model, thermal resistances R_{66}, R_{67}, R_{68}, R_{69}, R_{70}, R_{71} and R_{72} were included in the model to simulate heat transfer to the water channel. The thermal resistances were then simplified to include all the n_s slots, generating R_{73}, R_{74}, R_{75} and R_{76}. The definitions of the additional thermal resistances are described from Eq. (1) to Eq. (11), where h_{wa} is the cooling water heat transfer coefficient, l_u is the useful length of the stator core, b_s is the slot width, which is equal to the cooling channel width, k_{Cu} is the copper thermal conductivity, $\dot{m}_{wa}$ is the cooling water mass flow rate, c_p is the cooling water specific heat, b_d is the tooth width, h_{ch} is the cooling channel height, t_{ch} is the wall thickness of the cooling channel and k_{Fe} is the iron thermal conductivity. Materials' properties, such as k_{Cu} and k_{Fe}, are presented in Moghadam and Nejad (2020).

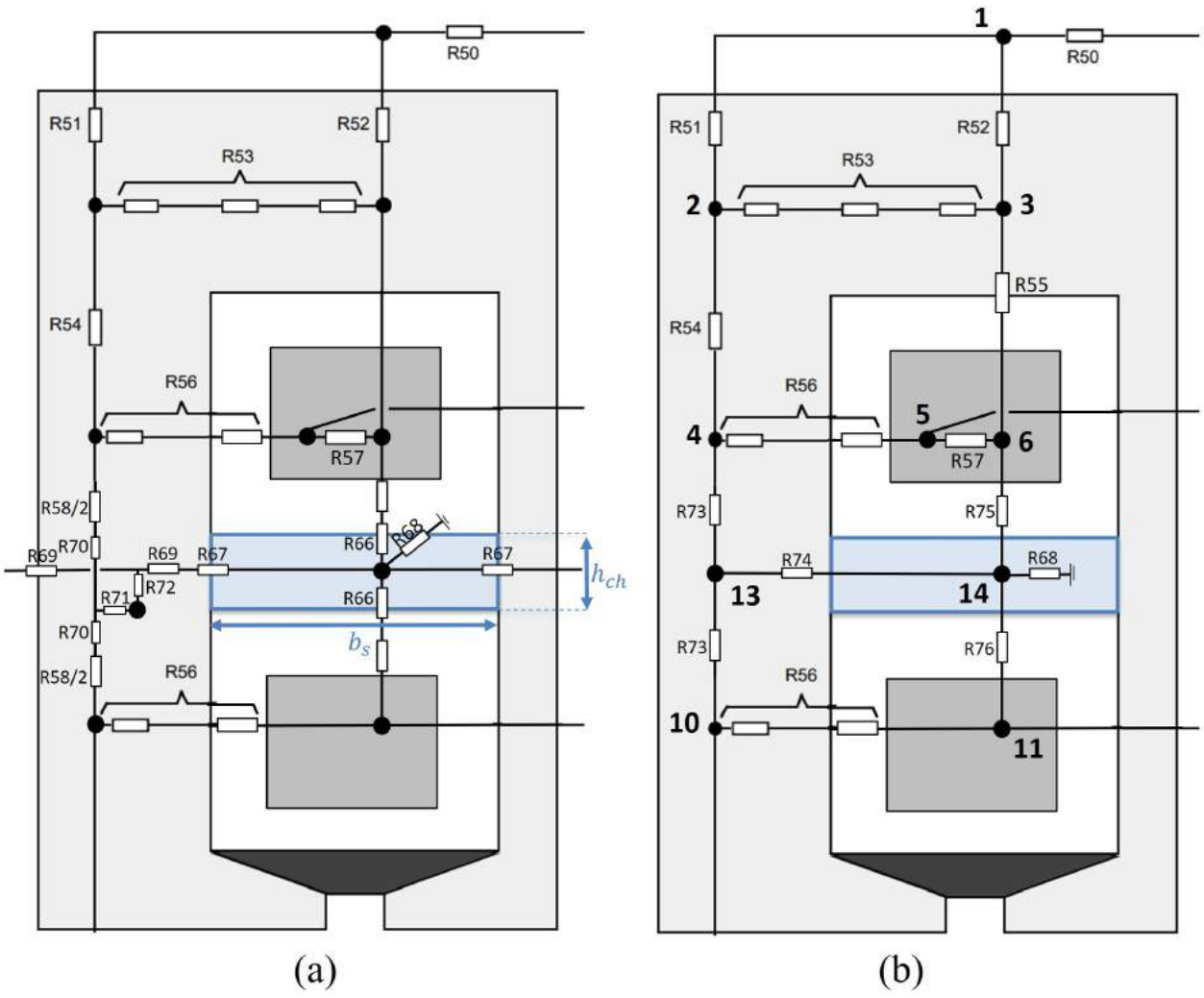

Figure 3. Representation of the proposed thermal thermal circuit: (a) detailed; (b) simplified.

$$R_{66} = \left(\frac{1}{h_{wa} l_u (b_s - 2t_{ch})} + \frac{t_{ch}}{k_{Cu} l_u b_s} \right) \tag{1}$$

$$R_{67} = \left(\frac{1}{h_{wa} l_u (h_{ch} - 2t_{ch})} + \frac{t_{ch}}{k_{Cu} l_u h_{ch}} \right) \tag{2}$$

$$R_{68} = \frac{1}{\dot{m}_{wa} c_p} \tag{3}$$

$$R_{69} = \frac{0.5 b_d}{h_{ch} l_u k_{Fe}} \tag{4}$$

$$R_{70} = \frac{0.5 h_{ch}}{b_d l_u k_{Fe}} \tag{5}$$

$$R_{71} = -\frac{1}{3} R_{70} \tag{6}$$

$$R_{72} = -\frac{1}{3} R_{69} \tag{7}$$

$$R_{73} = \frac{R_{58}/2 + R_{70}}{n_s} \tag{8}$$

$$R_{74} = \frac{R_{71} + R_{72} + 0.5(R_{67} + R_{69})}{n_s} \tag{9}$$

$$R_{75} = \frac{R_{66} + R_{13} + R_{11}}{n_s} \tag{10}$$

$$R_{76} = \frac{R_{66} + R_{13} + R_{11} + R_{20}}{n_s} \tag{11}$$

From the Grauers model, the thermal resistance R_{50} was changed to consider natural convection, according to Eq. (12), wherein h_{air} is the heat transfer natural convection coefficient, A_{ext} is the stator total cylindrical outer area and n_s is the number of slots. Churchill and Chu correlation (Churchill and Chu, 1975) was used to evaluate h_{air} at the reference temperature of 40 °C. The remaining resistances were left as the original model with external forced convection.

$$R_{50} = \frac{1}{h_{air}(A_{ext}/n_s)} \tag{12}$$

The Nusselt number, which is used to evaluate the cooling water heat transfer coefficient, was obtained using Gnielinski correlation (Gnielinski, 1976) for smooth tubes, as showed in Eq. (13).

$$Nu_D = \frac{(f/8)(Re_D - 1000)Pr}{1 + 12.7(f/8)^{1/2}(Pr^{2/3} - 1)} \tag{13}$$

where Pr is the cooling water Prandlt number and f is the friction factor for smooth surfaces, obtained by the equation, developed by Petukhov (Petukhov *et al.*, 1970). The cooling water properties were obtained using the mean temperature between the inlet and outlet temperature of a single pass.

3.3 Iterative model

An iterative thermal model was implemented since: (i) losses through copper are dependent from copper temperature; (ii) water properties are function of the water mean temperature inside the cooling channel, evaluated through channel exit temperature; (iii) air properties to evaluate natural convection parameters are dependent of stator outer surface temperature.

In this context, the parameters ΔT_{Cu}, ΔT_{water}, ΔT_{surf} are verified in each iteration, which are defined as the percent difference between the calculated temperature value and the value from the last iteration for copper mean temperature, cooling water mean temperature and stator outer surface temperature, respectively. The convergence criterion considered in this work was $\epsilon < 10^{-5}$. Copper mean temperature is defined as a weighted average between lower coil side, upper coil side and end winding, as described in Eq. (14), where l is the active length of the generator and l_b is the end winding length.

$$\bar{T}_{Cu} = \frac{l \cdot T_{Cu,lower} + l \cdot T_{Cu,upper} + 2l_b \cdot T_{Cu,end}}{2l + 2l_b} \tag{14}$$

Furthermore, the model was adapted to simulate thermal behavior considering multiple passes. This consideration was implemented setting the inlet water temperature of the cooling channel as the outlet temperature of the previous pass.

Figure 4 presents the algorithm of the iterative process. In essence, the model begins setting initial parameters, which are basically technical specifications and geometry dimensions. Then losses are evaluated setting an initial 150 °C mean copper temperature. Then, fluid properties and temperature field are evaluated and the iterative algorithm is performed for the first pass. In sequence, the model checks if the last pass $n_{pass,end}$ is already reached and if not, the pass number is increased and the inlet water temperature of the cooling channel $T_{in,water}(n_{pass})$ is eequal to as the outlet temperature of the previous pass $T_{out,water}(n_{pass} - 1)$. If the temperature field was evaluated for all passes, cooling water mass flow rate is increased and the process starts again. When calculations are performed for all mass flow rate values, reaching $\dot{m}_{max}$, the algorithm ends.

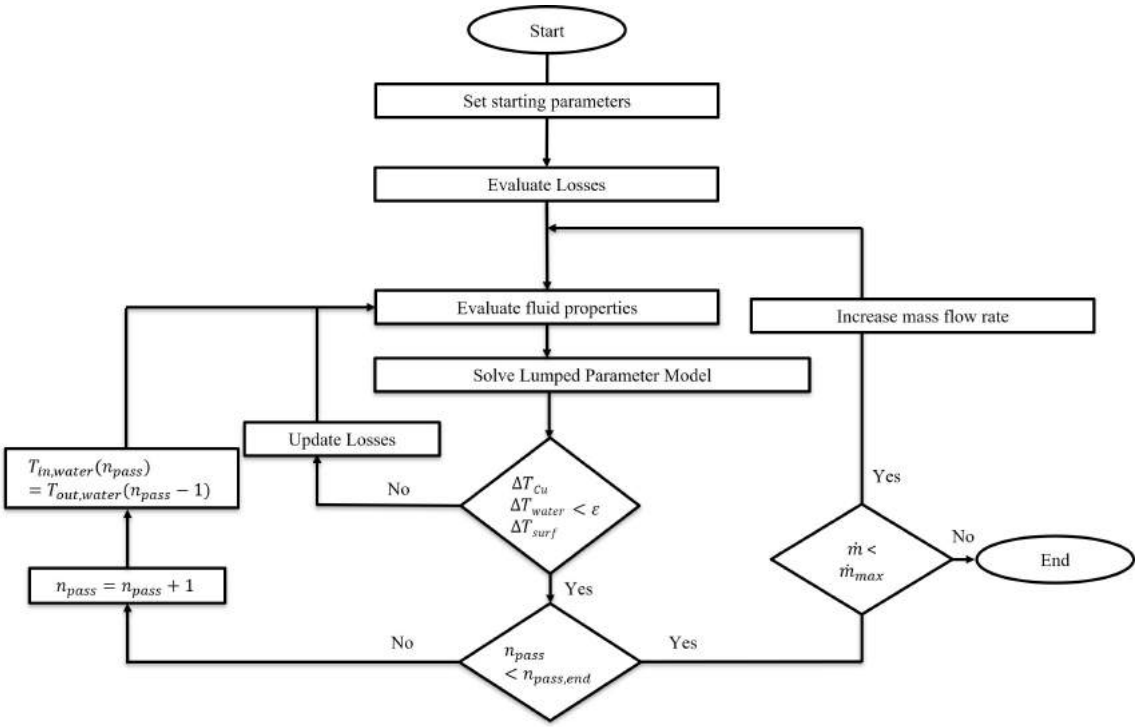

Figure 4. Thermal model flow chart.

4. RESULTS

Losses using external forced air convection are shown in Tab. 2, in which it can be seen that copper losses are predominant. The losses were used then as input to evaluate the temperature field through the LPN model without water cooling and considering an ambient temperature of 40 °C. The results are presented in Tab. 3. The hottest spots are end winding, lower and upper coil side, respectively.

Table 2. Losses evaluation applying model proposed by Grauers (1996).

Loss	**(kW)**
Copper	1017.20
Magnet	12.75
Iron (Stator yoke)	9.25
Iron (Teeth)	7.35
Windage	55.50
Aditional losses	3.32

Table 3. Temperature field applying model proposed by Grauers (1996)

Spot	**Temperature (°C)**
Stator cooling air	56.8
Stator yoke above a tooth	141.4
Stator yoke above a slot	143.3
Lower teeth	165.7
Upper teeth	179.9
Lower coil side	194.0
Upper coil side	213.0
End winding	233.8
Magnets	136.2
Internal air	95.2

External forced air convection for the studied 10 MW generator leads to extreme temperatures since end winding and

magnet results exceeds safe conditions, when considering a maximum copper temperature of 200 °C and demagnetization magnet temperature of 120 °C, as indicated by Grauers (1996) and Moghadam and Nejad (2020). Therefore a more effective cooling method is required.

In the proposed liquid cooling, two parameters were taken into account to analyze the system: the total water flow rate and the number of passes of the cooling coil. For a given flow rate value, the rise of the number of passes of the cooling coil increases the cooling water outlet temperature. On the other hand, it leads to a higher flow velocity inside the cooling channel, since the mass flow rate is divided between fewer cooling coils, and therefore affects fluid properties, such as the water heat transfer coefficient. In this context, Fig. (5) shows the influence of the number of passes on the temperature field and presents the end winding and magnet temperatures for the last pass of a cooling coil as function of cooling water flow rate, considering four designed cooling systems with 5, 10, 15 and 20 number of passes.

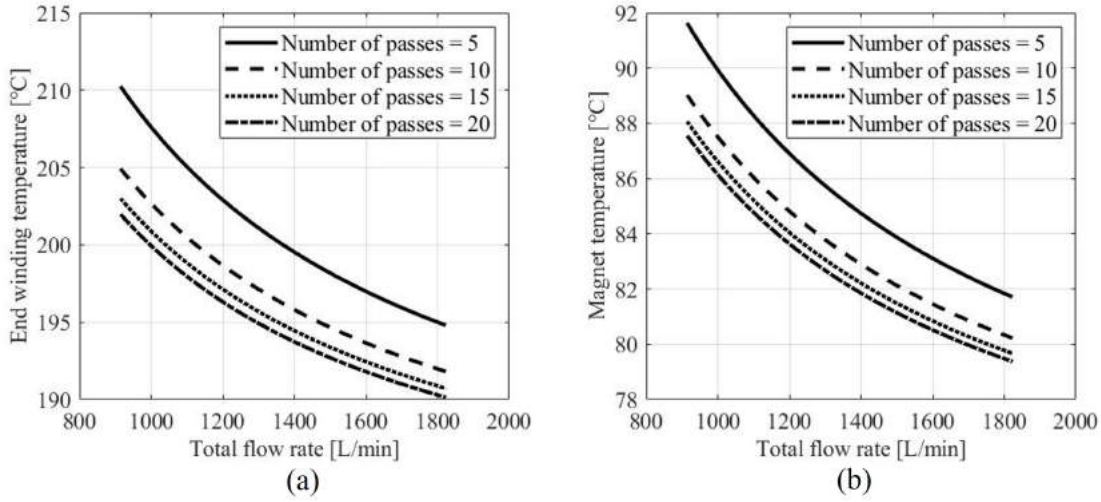

Figure 5. Last pass temperature for different pass number designs: (a) end winding; (b) permanent magnet.

The temperature of the last pass is analyzed since it results in the highest temperatures. According to Fig. (5), the higher the number of passes, the lower the temperatures at the points of interest, even though its effectiveness on reducing temperature decreases over the number of passes. This behavior can be seen in Fig. (6), in which a 1600 L/min flow rate is fixed and the end winding and magnet temperatures are expressed as a function of the designed number of passes. In this case, it can be stated that coils with more than 20 passes have no significant impact on temperature reduction.

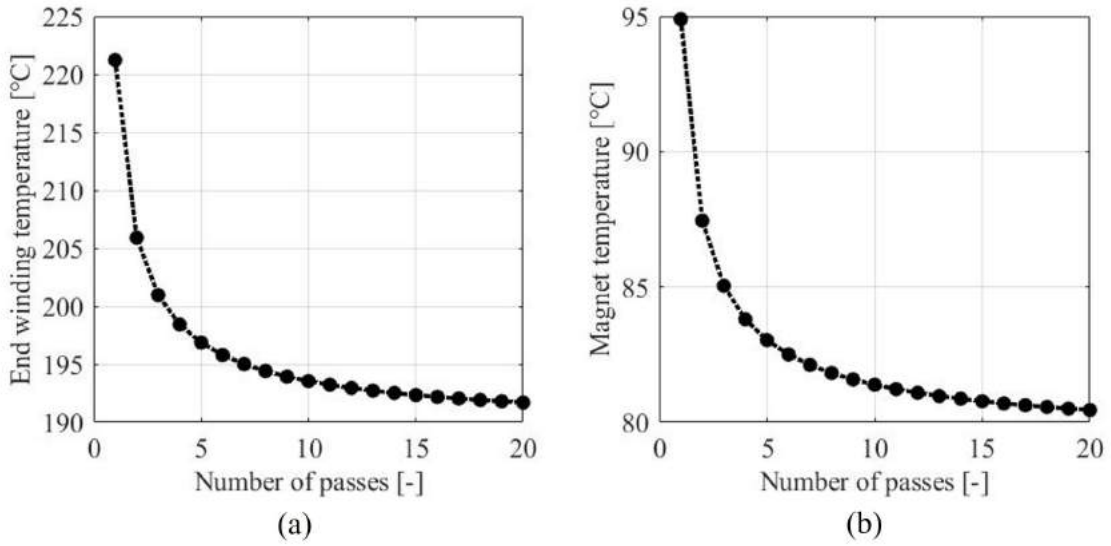

Figure 6. Last pass temperature for different pass number design considering a 1600 L/min flow rate: (a) End winding; (b) Magnet.

Figure (7) shows the temperature behavior of the outlet cooling water channel and mean copper temperature for each

pass, considering a designed generator with 20 passes and four different total flow rates. Temperature rise for both cases has a linear behavior, since losses remain practically constant and water properties do not vary significantly for each pass, which leads to an almost constant heat transfer coefficient. Therefore, the temperature increase vector, output of the LPN model, remains nearly constant and consequently all spots evaluated through the model present the same linear behavior. Figure (7) also shows that lower flow rates cause higher temperature increase, because of lower mean velocity inside the cooling channel.

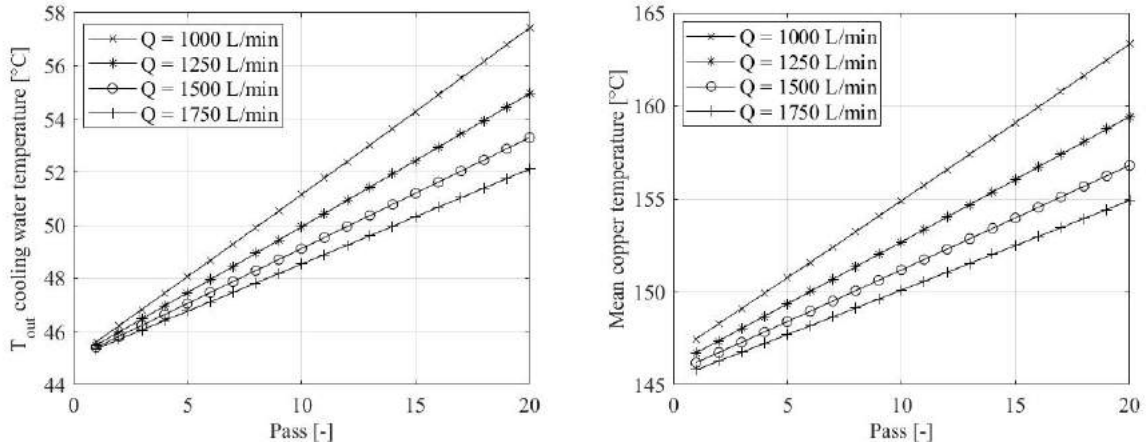

Figure 7. Outlet channel cooling water temperature (a) and mean copper temperature (b) for each pass.

Fig. (8) shows the total losses and the average copper temperature in function of the water flow rate for a generator with 20 passes. As introduced in section 3, copper losses are a function of its temperature and armature current. Therefore the graphs in Fig. (8a) and Fig. (8b) are quite similar, confirming the correlation between losses and copper temperature.

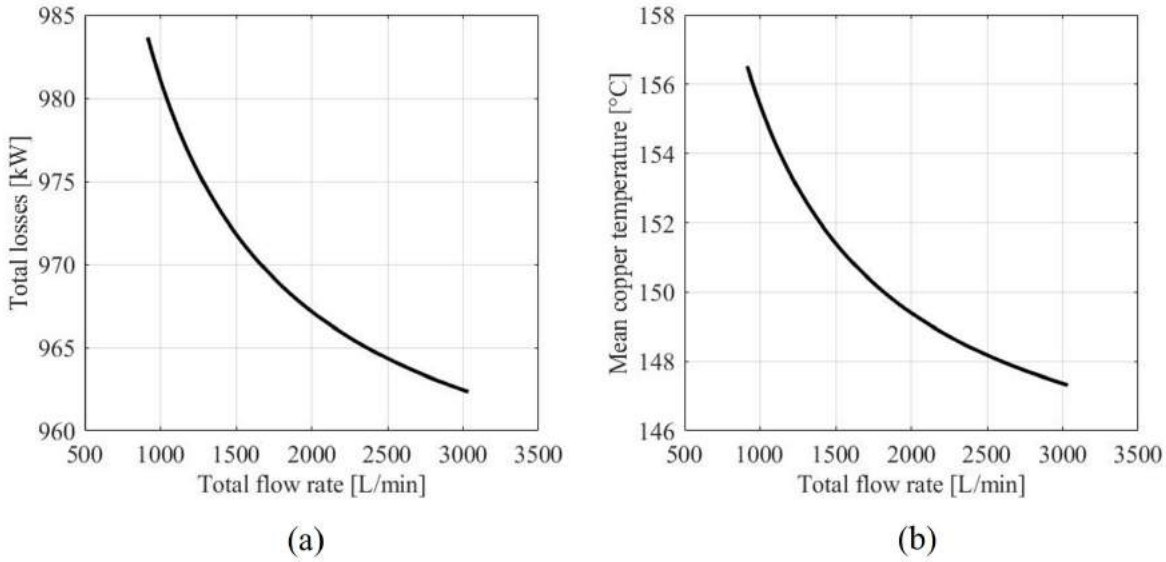

Figure 8. (a) Average total losses and (b) Average mean copper temperature.

Even though direct cooling can lower the copper temperature, its losses remain significant, since they are dependent on the square of armature current density. Therefore, decreasing winding temperature presents a nonsignificant impact on improving generator efficiency, which can be seen in Fig. (9), which shows the poorly impact in this range of the cooling water flow rate on generator efficiency.

5. CONCLUSIONS

High power wind generators present very complex challenges in thermal control because of their geometrical parameters and high current density. The thermal management in these systems is indispensable to ensure reliability and to reduce power losses. Here, thermal modeling of a 10 MW DD-PMSG was performed on the basis of the lumped

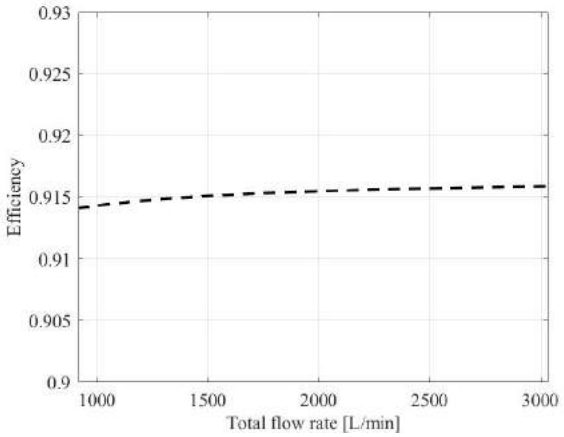

Figure 9. Efficiency as function of flow rate.

parameter network to carry out steady-state simulations.

Direct cooling performs better than external forced air convection on stator surface when lower temperatures need to be achieved, mostly by high power generators. A multiple-pass cooling system is an adequate solution to achieve temperature requirements with lower flow rates. According to simulation results, a generator with 20 passes and 1600 L/min flow rate achieves the thermal requirements and presents electrical efficiency of about 91.5 %.

For further works, the authors recommend a numerical study to evaluate temperature fields in the studied generator and eventually the construction of an experimental model to validate the simulation results and investigate the uncertainties in the LPN thermal model. Also, studies about the pressure losses inside the channels should be performed to estimate the energy for pumping the cooling fluid.

6. ACKNOWLEDGEMENTS

The authors acknowledge Petrobras S.A. for the scholarship from the P&D project "Avaliação da Interligação de uma Geração Eólica Offshore a um Sistema Elétrico de 13,8 kV Típico de uma UEP de Libra".

7. REFERENCES

Alexandrova, Y., Semken, R.S. and Pyrhönen, J., 2014. "Permanent magnet synchronous generator design solution for large direct-drive wind turbines: Thermal behavior of the lc dd-pmsg". *Applied Thermal Engineering*, Vol. 65, pp. 554–563.

Bazzo, T., Carlson, R. and Wurtz, F., 2015. "Wind power pmsg optimally designed for maximum energy proceeds and minimum cost". In *IEEE International Symposium on Industrial Electronics*. Búzios, RJ, Brazil.

Churchill, S.W. and Chu, H.H.S., 1975. "Correlating equations for laminar and turbulent free convection from a horizontal cylinder". *International Journal of Heat and Mass Transfer*, Vol. 18, pp. 1049–1053.

Fan, J., Tian, Y., Xing, Z., Qi, F., Li, D. and Deng, L., 2019. "Design and analysis of cooling system for 3.2mw split-type permanent magnet direct-driven wind turbine generator". In *2019 22nd International Conference on Electrical Machines and Systems (ICEMS)*. Harbin, China.

Gnielinski, V., 1976. "New equations for heat and mass transfer in turbulent pipe and channel flow". *International Chemical Engineering*, Vol. 16, p. 359.

Grauers, A., 1996. *Design of Direct-driven Permanent-magnet Generators for Wind Turbines*. Ph.D. thesis, School of Electrical and Computer Engineering, Chalmers University of Technology, Göteborg.

GWEC, 2021. "Global wind report 2021". Global Wind Energy Council, Brussels, www.gwec.net. Accessed 12 January 2021.

Jiang, Y., 2010. *Wind turbine cooling technologies*. WIT Transactions on State of the Art in Science and Engineering, Southampton.

Moghadam, F.K. and Nejad, A.R., 2020. "Evaluation of pmsg-based drivetrain technologies for 10-mw floating offshore wind turbines: Pros and cons in a life cycle perspective". *Wind Energy*, Vol. 23, pp. 1542–1563.

Petukhov, B.S., Irvine, T.F. and Hartnett, J.P., 1970. *Advances in Heat Transfer*. Academic Press, New York.

8. RESPONSIBILITY NOTICE

The authors are solely responsible for the printed material included in this paper.